Pergamon

Int. J. Solids Structures Vol. 32, No. 10, pp. 1349–1369, 1995

0020-7683/95 $9.50 + .00

0020-7683(94)00204-5

MODAL INTERACTION IN COMPOSITE CYLINDERS UNDER HYDROSTATIC PRESSURE

AKIHITO KASAGI† and SRINIVASAN SRIDHARAN
Washington University, Campus Box 1130, St. Louis, MO 63130, U.S.A.

(*Received* 25 *March* 1994; *in revised form* 20 *August* 1994)

Abstract—A novel and computationally effective procedure for the study of the overall and local instabilities in composite ring stiffened shells subjected to hydrostatic pressure is presented. The key feature of the formulation employed is a judicious combination of Koiter's amplitude modulation technique and the Byskov–Hutchinson asymptotic procedure for the interactive buckling analysis.

A potential energy function is formulated in terms of a comparatively small number of degrees-of-freedom, *viz.* the degrees-of-freedom depicting the amplitude modulating function and a scaling factor of the overall buckling mode. As a result of the amplitude modulation, there arise in the potential energy function non-vanishing cubic interactive terms which control the process of mode interaction. Imperfection-sensitivity under coincident buckling is examined. It appears that a 50% reduction of the buckling capacity must probably be allowed for as a result of modal interaction under near-coincident buckling. The optimality under interactive buckling is also examined with the total volume of the material kept constant and the critical stress ratio varied.

NOTATION

$[C]$, C_{ij}, C_{ij}	constitutive relations
d	stiffener depth
h	shell thickness
L	shell length
L_1, L_{11}, L_2	linear, bilinear and quadratic operators respectively
m, n	number of circumferential waves for the overall and local modes of buckling respectively
N_s	number of stiffeners
P	axial force
Q_3, Q_4, Q_{mix}	cubic, quartic and the mixed second order terms, respectively, in the potential energy function
q_0	external lateral pressure
R_0, R_1	inner and outer radii of shell
R	middle radius of shell $= (R_0 + R_1)/2$
r, θ, x	radial, circumferential and longitudinal directions respectively in cylindrical coordinates
S_p	stiffener spacing
t_s	stiffener thickness
u, v, w	displacement components in the longitudinal, circumferential and radial directions respectively
ε_x, ε_θ, ε_r	normal strain components
$\gamma_{r\theta}$, γ_{rx}, $\gamma_{\theta x}$	(engineering) shear strain components
ζ, η	natural coordinates in the radial and longitudinal directions
ξ, λ	scaling factor and load parameter
λ_{cr}	critical pressure
$\lambda^{(2)}$	postbuckling coefficient
λ_1, λ_2	classical overall and local buckling pressures respectively
$\lambda_{\max}$	maximum load carrying capacity
$\bar{\xi}_1$, $\bar{\xi}_2$	imperfection parameters for overall and local modes respectively
Ξ_1	$= \bar{\xi}_1/R$
Ξ_2	$= \bar{\xi}_2/h$
Π	potential energy function
$(\ldots)^{(0)}$	prebuckling quantities
$(\ldots)^{(1)}$	first order field quantities
$(\ldots)^{(2)}$	second order field quantities
$(\ldots)_1$	quantities of the overall mode
$(\ldots)_2$	quantities of the local mode
$(\ldots)_{12}$	quantities of the mixed second order field.

1. INTRODUCTION

The rapidly increasing use of high-performance composite materials in the fabrication of structural components and systems has provided the motivation for vigorous and sus-

† Current address: Kozo Keikau Engineering Inc., 38-13, 4-Chome, Hon-cho, Nakano-ku, Tokyo, Japan.

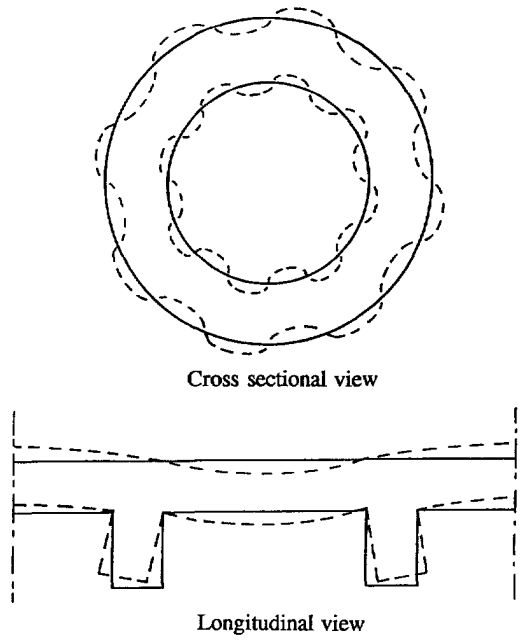

Fig. 1(a). Local mode of buckling.

tained research in this field for the past several decades. In recent times there has been considerable interest in the structural instability of relatively thick composite shells. However, far greater attention has been given to initial buckling (Kardomateas, 1993; Simitses *et al.*, 1992, 1993) than to the problems of postbuckling and nonlinear modal interaction. A search for an optimal design of composite cylindrical shells, of the type proposed to be used as submarine vessels, leads to a geometry for which buckling and the accompanying nonlinear behavior are of major concern. These shells are usually, in the interests of economy and lightness, reinforced best by ring stiffeners to resist severe hydrostatic pressure. Such stiffened shells can suffer buckling not only in the overall sense, but also locally between stiffeners. These two distinctive buckling modes which dominate the behavior of ring stiffened shells are described as follows:

(i) The short wave local buckling shown in Fig. 1(a) in which buckling occurs between stiffeners forming several half waves in the circumferential direction. The nodes of buckling waves in the longitudinal direction coincide with the position of stiffeners so that the role of stiffeners may be viewed as a support which arrests the movement of the shell in the radial direction. But, this involves bending action of stiffeners as a result of buckling.

(ii) The long wave overall buckling as shown in Fig. 1(b) where the stiffeners are pulled radially in and out; the mode would consist of a small number of waves in the circumferential direction.

It is well known that the adverse nonlinear mode interaction between these modes is the principal cause of failure of an optimally designed shell structure for which the critical stresses corresponding to these modes would be close. Thus, it is essential to understand the nature of response such as possible postbuckling resistance or imperfection-sensitivity and the interaction of overall and local instabilities.

The question of optimal design of stiffened structures in conjunction with interaction between local and overall buckling has been raised several times over the last three decades. A classical criterion of optimization is that the overall and local critical loads should coincide. Koiter and Skaloud (1963) pointed out that such designs can lead to significant imperfection-sensitivity. The works done by van der Neut (1969) and Tvergaard (1973) are regarded as among the significant contributions to the imperfection-sensitivity arising out

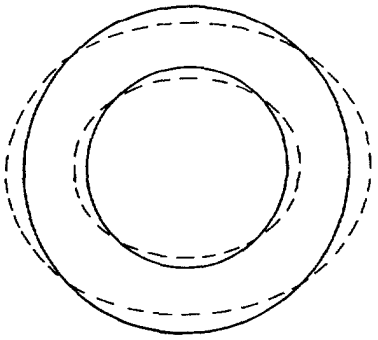

Cross sectional view

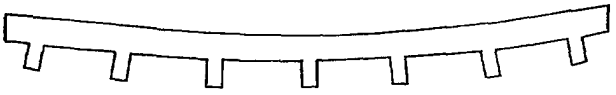

Longitudinal view

Fig. 1(b). Overall mode of buckling.

of the interaction for built-up columns and stiffened plates. Koiter and Pignataro (1976a,b) developed a sophisticated, if somewhat simplified analytical procedure for the study of interactive buckling of axially compressed stiffened shells. They introduced the concept of amplitude modulation, which accounts for the slowly varying amplitude of local buckling around the shell and neglected in their analysis the mixed second order field (m.s.o.f.) which arises by the interaction overall and local modes of buckling. It is only recently that the full implications of this approach have been widely understood. It is now appreciated (see for example, Sridharan and Peng, 1989) that the amplitude modulation performs the role of accounting for a family of secondary local modes triggered in the interaction and effectively takes over the role of the m.s.o.f. Byskov and Hutchinson (1977) pioneered an asymptotic approach to the analysis of interactive buckling problems wherein the critical loads may be close or well separated. Their analysis yielded spectra of imperfection-sensitivity of axially compressed stringer-stiffened shells. The optimization of the load carrying capacity is discussed with reference to these spectra. Significant reduction of load carrying capacity is noticed at near coincident critical loads. In their analysis, Byskov and Hutchinson make an intuitive choice of the functions characterizing the m.s.o.f. as a product of local and overall mode and examine the influence of possible singularities in the evaluation of this field. Though subsequent studies have shown their results to be sufficiently accurate (Byskov and Hansen, 1980; Byskov *et al.*, 1988), it must be emphasized that the evaluation of the m.s.o.f. in two mode local–overall mode interaction problems is, in general, riddled with singularities. Hui (1985) has compared the results of the asymptotic procedure (Byskov and Hutchinson, 1977) and Koiter's amplitude modulation theory and concluded that in two-mode interactive buckling problems, the amplitude modulation theory is generally superior to the asymptotic method due to computational simplicity, and validity for a large range of imperfection magnitudes.

The present study deals with the interactive buckling of ring stiffened shells under hydrostatic pressure. The objective here is to develop a simple yet realistic model that can capture the essential features of structural behavior associated with nonlinear modal

interaction. Particular attention is given to modeling layered composite shells. A computationally inexpensive model, both in terms of user effort and computation time, could play a crucial role in the more advanced stages of design and in particular in developing a powerful optimization strategy. This is sought to be achieved through the use of (i) an axisymmetric solid element which employs exact trigonometric displacement functions for the circumferential direction and p-version type polynomial functions (Szabó and Babuska, 1991) in the other two orthogonal directions and (ii) a judicious combination of an asymptotic procedure and the amplitude modulation technique.

In the present strategy, as in the asymptotic approach, the local and the overall modes are first treated individually in order to determine the respective buckling modes and associated second order fields before proceeding with the interactive buckling analysis. The potential energy function governing the modal interaction is then simply expressed in terms of the amplitude of overall mode (one degree-of-freedom) and the degrees-of-freedom depicting the modulating function associated with the local mode. This makes it possible to reduce the computational effort considerably in comparison to a conventional multimodal analysis. The concept and the necessity of amplitude modulation of rotationally symmetric shell structures are revisited in the context of the present problem and shown to be fully justified in a systematic application for the theory of modal interaction. Numerical examples are presented to illustrate the imperfection-sensitivity of the shells with coincident and well separated critical pressures, the relative importance of the various interactive terms in the potential energy function, and the salient features of the structural response of the shells under modal interaction.

Often, in a simply supported shell, the local buckling tends to remain localized near the edges. This is the result of prebuckling axisymmetric deformations which are concentrated near the edges. In practice this can, however, be eliminated by appropriate local thickening of the shell. Thus from the view point of interaction such a localized mode is of little interest and will not be considered in the present study.

2. METHODOLOGY

2.1. *Constitutive relations*

Consider a curved lamina whose principal material directions are defined by the coordinate system 1–2–3 where axis 3 coincides with the outward normal at any point, and axes 1 and 2 are obtained by rotating the tangents in the longitudinal and radial directions through an angle α. The global coordinate system at any point is defined by the longitudinal (x-axis), circumferential (θ-axis) and radial (r-axis) as shown in Fig. 2(a) and the corresponding displacement components are respectively u, v and w. Similarly the material principal axes of a ring stiffener are defined analogously by referring to Fig. 2(b). The relationship between stresses and strains with reference to the global coordinate system takes the form:

$$\begin{Bmatrix} \sigma_1 \\ \sigma_2 \\ \sigma_3 \\ \sigma_4 \\ \sigma_5 \\ \sigma_6 \end{Bmatrix} = \begin{bmatrix} C_{11} & C_{12} & C_{13} & 0 & 0 & C_{16} \\ C_{12} & C_{22} & C_{23} & 0 & 0 & C_{26} \\ C_{13} & C_{23} & C_{33} & 0 & 0 & C_{36} \\ 0 & 0 & 0 & C_{44} & C_{45} & 0 \\ 0 & 0 & 0 & C_{45} & C_{55} & 0 \\ C_{16} & C_{26} & C_{36} & 0 & 0 & C_{66} \end{bmatrix} \begin{Bmatrix} \varepsilon_1 \\ \varepsilon_2 \\ \varepsilon_3 \\ \varepsilon_4 \\ \varepsilon_5 \\ \varepsilon_6 \end{Bmatrix}. \tag{1a–f}$$

Equation (1a–f) is expressed as:

$$\sigma_i = C_{ij}\varepsilon_j \quad (i,j = 1,2,\ldots,6). \tag{2}$$

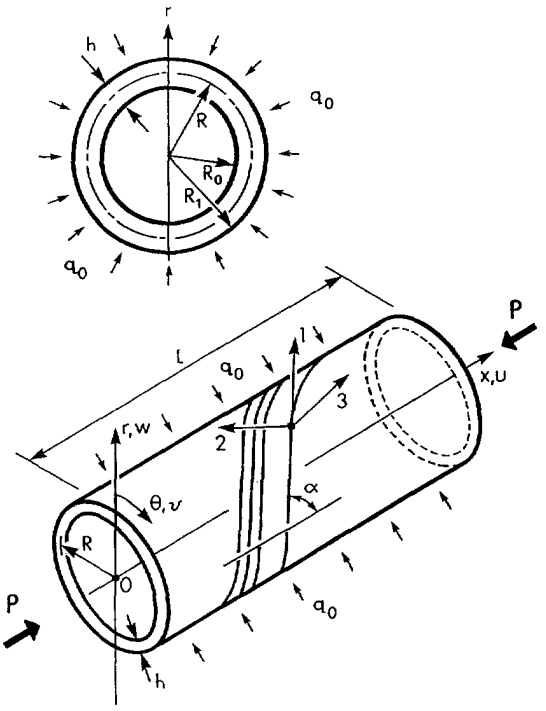

Fig. 2(a). Shell geometry and sign convention for fiber orientation.

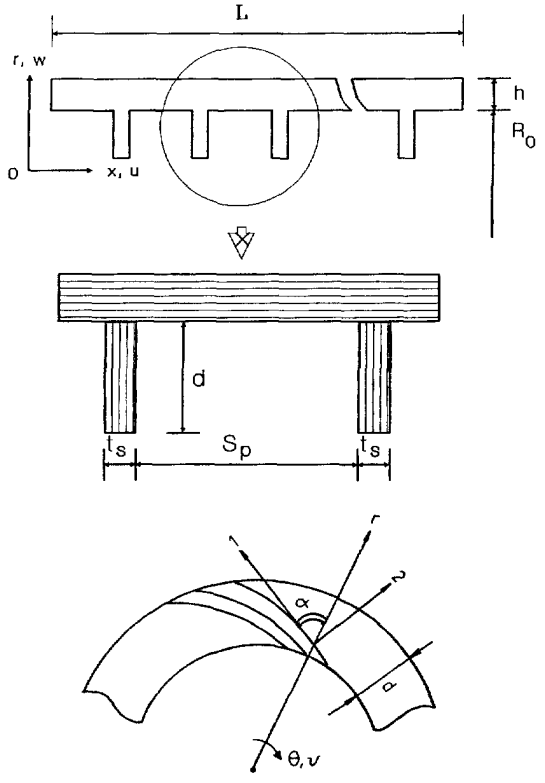

Fig. 2(b). Geometry of ring stiffener.

Arabic subscripts 1 6 are defined as follows:
for the shell:

$$1 \to xx, \quad 2 \to \theta\theta, \quad 3 \to rr, \quad 4 \to r\theta, \quad 5 \to rx, \quad 6 \to \theta x \tag{3a}$$

for the stiffener:

$$1 \to rr, \quad 2 \to \theta\theta, \quad 3 \to xx, \quad 4 \to \theta x, \quad 5 \to rx, \quad 6 \to r\theta. \tag{3b}$$

The coefficients of eqn (1a–f) are obtainable at any location by a transformation to the axes of the structure, of the elastic constants referred to the principal material axes (Jones, 1975). Further, in order to improve the numerical conditioning, we set, for stiffeners, σ_{xx} (the normal stress in the thickness direction) = 0. From eqn (1c) in conjunction with the notation in eqn (3b), we obtain the following equation:

$$C_{13}\varepsilon_{rr} + C_{23}\varepsilon_{\theta\theta} + C_{33}\varepsilon_{xx} + C_{36}\gamma_{r\theta} = 0 \tag{4a}$$

from which,

$$\varepsilon_{xx} = -\frac{1}{C_{33}}(C_{13}\varepsilon_{rr} + C_{23}\varepsilon_{\theta\theta} + C_{36}\gamma_{r\theta}) \tag{4b}$$

and re-substituting into the constitutive relations, we establish the result:

$$\tilde{C}_{ij} = C_{ij} - \frac{C_{i3}}{C_{33}}C_{3j} \quad (i,j = 1,2,6); \quad \tilde{C}_{ij} = C_{ij}\,(i,j = 4,5) \tag{5}$$

where C_{ij} represents the reduced stiffness introduced. An Arabic subscript 3 for the stiffener is absent throughout in the present treatment.

2.2. *Deformation contribution from individual buckling modes*

Displacement fields and strain–displacement relations. We define the displacement vector given by:

$$\{\mathrm{u}\} = \{u_1\ u_2\ u_3\} \equiv \{u\ v\ w\}. \tag{6}$$

An asymptotic expansion of the displacement fields may be written in the form of power series in a scaling parameter ξ which measures the buckled state,

$$\{\mathrm{u}\} = \lambda\{\mathrm{u}^{(0)}\} + \{\mathrm{u}^{(1)}\}\xi + \{\mathrm{u}^{(2)}\}\xi^2 + \{\mathrm{u}^{(3)}\}\xi^3 + \ldots \tag{7}$$

where λ is the load parameter. The superscript "(0)" refers to the linear unbuckled equilibrium path, the $\{\mathrm{u}^{(1)}\}$ (first order field) is given by the buckling mode while the term $\{\mathrm{u}^{(2)}\}$ is the second order field and so on. The present study considers up to the second order field to predict the initial postbuckling response. Similar expressions may be written for the strains $\{\varepsilon\}$ and stresses $\{\sigma\}$.

Strain–displacement relations employed are based on three-dimensional elasticity (Ambartsumyan, 1970). Strains are considered to be infinitesimally small, but displacements and their gradients can be large. In the nonlinear part of strain–displacement relations for the shell part, the displacement gradients in the r-direction are assumed to be very small in comparison to the others. Thus they are safely neglected.

For the shell skin:

$$\varepsilon_{rr} = \frac{\partial w}{\partial r} \qquad \gamma_{\theta x} = \frac{\partial v}{\partial x} + \frac{1}{r}\frac{\partial u}{\partial \theta} + \frac{1}{r}\left[\left(\frac{\partial w}{\partial \theta} - v\right)\left(\frac{\partial w}{\partial x}\right) + w\left(\frac{\partial v}{\partial x}\right)\right]$$

$$\varepsilon_{\theta\theta} = \frac{1}{r}\frac{\partial v}{\partial \theta} + \frac{w}{r} + \frac{1}{2r^2}\left[\left(\frac{\partial w}{\partial \theta} - v\right)^2 + \left(\frac{\partial v}{\partial \theta} + w\right)^2\right] \qquad \gamma_{rx} = \frac{\partial u}{\partial r} + \frac{\partial w}{\partial x}$$

$$\varepsilon_{xx} = \frac{\partial u}{\partial x} + \frac{1}{2}\left(\frac{\partial w}{\partial x}\right)^2 \qquad \gamma_{r\theta} = \frac{1}{r}\frac{\partial w}{\partial \theta} + \frac{\partial v}{\partial r} - \frac{v}{r} \tag{8a–f}$$

for the stiffener:

$$\varepsilon_{rr} = \frac{\partial w}{\partial r} + \frac{1}{2}\left[\left(\frac{\partial u}{\partial r}\right)^2 + \left(\frac{\partial w}{\partial r}\right)^2\right] \qquad \gamma_{\theta x} + \frac{\partial v}{\partial x} + \frac{1}{r}\frac{\partial u}{\partial \theta}$$

$$\varepsilon_{\theta\theta} = \frac{1}{r}\frac{\partial v}{\partial \theta} + \frac{w}{r} + \frac{1}{2r^2}\left[\left(\frac{\partial u}{\partial \theta}\right)^2 + \left(\frac{\partial w}{\partial \theta}\right)^2\right] \qquad \gamma_{rx} = \frac{\partial u}{\partial r} + \frac{\partial w}{\partial x}. \tag{9a–e}$$

$$\gamma_{r\theta} = \frac{1}{r}\frac{\partial w}{\partial \theta} + \frac{\partial v}{\partial r} - \frac{v}{r} + \frac{1}{r}\left[\left(\frac{\partial u}{\partial r}\right)\left(\frac{\partial u}{\partial \theta}\right) + \left(\frac{\partial w}{\partial r}\right)\left(\frac{\partial w}{\partial \theta}\right)\right]$$

Strain–displacement relations in eqns (8a–f) and (9a–e) may be expressed in the general form using linear L_1 and quadratic L_2 operators:

$$\varepsilon_i = L_{1_{ij}}(u_j) + \tfrac{1}{2}L_{2_{ij}}(u_j). \quad (i = 1,2,\ldots,6; \quad j = 1,2,3). \tag{10}$$

Prebuckling analysis. The prebuckling path is treated as linear in the sense,

$$L_{11_i}(u_j^{(0)}, v_j) = 0 \tag{11a}$$

for all i and j and any v_j; and L_{11} is a bilinear operator, given by:

$$L_2(u+v) = L_2(u) + 2L_{11}(u,v) + L_2(v). \tag{11b}$$

The displacement field is axisymmetric in the sense that it is independent of θ coordinate. This is discussed in some detail elsewhere (Kasagi, 1994; Kasagi and Sridharan, 1994). In the buckling analysis that is described in the next section, the only stress components that are required are ϕ_{xx}, $\sigma_{\theta\theta}$ and $\tau_{\theta x}$ for the shell skin and only $\sigma_{\theta\theta}$ for the stiffeners.

Determination of the first and second order fields. For the case of linear prebuckling paths, the potential energy functions for the first and second order fields may be written in the form (Kasagi and Sridharan, 1993):

$$\Pi^{(1)} = \tfrac{1}{2}[C_{ij}L_{1_{ik}}(u_k^{(1)}) \cdot L_{1_{jl}}(u_l^{(1)}) + \lambda\,\sigma_i^{(0)} \cdot L_{2_{ik}}(u_k^{(1)})] + \lambda\,\Omega^{(1)}$$

$$\Pi^{(2)} = \tfrac{1}{2}[C_{ij}L_{1_{ik}}(u_k^{(2)}) \cdot L_{1_{jl}}(u_l^{(2)}) + \lambda\,\sigma_i^{(0)} \cdot L_{2_{ik}}(u_k^{(2)})$$

$$+ C_{ij}\{L_{2_{ik}}(u_k^{(1)}) \cdot L_{1_{jl}}(u_l^{(2)}) + 2L_{1_{ik}}(u_k^{(1)}) \cdot L_{11_j}(u_l^{(1)}, u_l^{(2)})\}] + \lambda\,\Omega^{(2)} \tag{12a–b}$$

$$(i,j = 1,2,\ldots,6; \quad k,l = 1,2,3).$$

In the above, the term Ω is a quadratic function which takes into account the 'fluid pressure

loading' discussed by Koiter (1967) and elsewhere (see Appendix A). The displacement functions describing the first and second order fields take the following forms:

$$u_k^{(1)} = u_{kij}^{1S}\,\Phi_i(\zeta)\Phi_j(\eta)\sin(n\theta) + u_{kij}^{1C}\,\Phi_i(\zeta)\Phi_j(\eta)\cos(n\theta)$$

$$u_k^{(2)} = u_{kij}^{20}\,\Phi_i(\zeta)\Phi_j(\eta) + u_{kij}^{2S}\,\Phi_i(\zeta)\Phi_j(\eta)\sin(2n\theta) + u_{kij}^{2C}\,\Phi_i(\zeta)\Phi_j(\eta)\cos(2n\theta) \qquad (13a\text{–}b)$$

$$(i = 1, 2, \ldots, p_r + 1;\quad j = 1, 2, \ldots p_x + 1;\quad k = 1, 2, 3)$$

where the $\phi_i(\zeta)$ and $\phi_j(\eta)$ are shape functions proposed by Szabó and Babuska (1991) and summarized in Appendix B; p_r and p_x stand for polynomial levels which are independently selected for radial and longitudinal directions respectively. In general the order of the p-levels for the first and second order displacement fields are independently selected. Equations of equilibrium are obtained by rendering the appropriate potential energy functions stationary. Equation (12a) leads to the linear eigenvalue problem for critical pressure λ_{cr} and the associated buckling mode, while eqn (12b) yields a system of linear simultaneous equations. λ is set equal to λ_{cr} in the solution of the second order field problem.

With the displacement fields thus obtained, it is possible study the response in individual modes, i.e. in the absence of interaction. The potential energy function for the perfect structure takes the form:

$$\Pi = \tfrac{1}{2}(\mathrm{a} - \lambda \mathrm{b})\xi^2 + \mathrm{d}\xi^4. \qquad (14a)$$

The equilibrium equation describing the buckled state can then be obtained as:

$$\frac{\lambda}{\lambda_{cr}} = 1 + \lambda^{(2)}\left(\frac{\xi}{h}\right)^2 \quad \text{with} \quad \lambda_{cr} = \frac{a}{b};\quad \lambda^{(2)} = 4h^2\frac{d}{a}. \qquad (14b)$$

The constants a, b and d are computed on the basis of a buckling mode which is normalized by prescribing the amplitude at the mid-section of the shell to be unity and ξ, the scaling parameter is identified with this the critical load in the presence of imperfections. Koiter (1945) has shown that if $\bar{\xi}$ is a measure of the imperfection in the form of the buckling mode and is defined in the same sense as ξ, then an asymptotic estimate of the maximum load is given by the solution to the cubic equation:

$$\sqrt{(1-S)^3} = \frac{3\sqrt{3}}{2}\sqrt{-\lambda^{(2)}}\left|\frac{\bar{\xi}}{h}\right| S \qquad (15)$$

where $S = \lambda_{max}/\lambda$ and $\lambda^{(2)} \leqslant 0$.

A study of single mode postbuckling analysis of cylindrical shells has been presented by the authors in an earlier paper (Kasagi and Sridharan, 1993, 1994).

2.3. *Interactive buckling analysis*

Concept of amplitude modulation. As a consequence of the interaction of the overall mode with the local mode, additional patterns of deformation are generated. These are given to the first order of accuracy by the mixed second order field. In this section we shall treat the overall buckling mode as a "slowly varying" function (Koiter and Pignataro, 1976a). An asymptotic expansion of the displacement fields for the interactive buckling problem may be written in the following manner (Byskov and Hutchinson, 1977):

$$\{u\} = \{u^{(0)}\} + \{u_1^{(1)}\}\xi_1 + \{u_2^{(1)}\}\xi_2 + \{u_1^{(2)}\}\xi_1^2 + \{u_{12}^{(2)}\}\xi_1\xi_2 + \{u_2^{(2)}\}\xi_2^2 + \ldots \qquad (16)$$

where the subscripts 1 and 2 represent overall buckling quantities and local ones respectively, and $u_{12}^{(2)}$ is termed the mixed second order field. In the following discussion we consider the

case of a specially orthotropic shell for the sake of conciseness. Each of the buckling modes is taken as:

$$\begin{aligned} u_1^{(1)} &= u_m(x)\cos(m\theta) & u_2^{(1)} &= u_n(x)\cos(n\theta) \\ v_1^{(1)} &= v_m(x)\sin(m\theta) & v_2^{(1)} &= v_n(x)\sin(n\theta) \\ w_1^{(1)} &= w_m(x)\cos(m\theta) & w_2^{(1)} &= w_n(x)\cos(n\theta) \end{aligned} \qquad \begin{matrix} \text{(no sum on } m \text{ or } n) \\ (n\ m) \end{matrix} \tag{17}$$

where m and n stand for wave number. These expressions are substituted into the appropriate nonlinear differential equations of equilibrium and the coefficients of $\xi_1\xi_2$ on each side matched for each of the equations. In order to illustrate the essential features of the field, we shall make some drastic simplifications in this discussion. Thus using Donnell type theory (Brush and Almroth, 1975) and setting all the displacement gradients of the "slowly varying" overall mode to zero, the equilibrium equation in the transverse direction for the mixed second order field is written as:

$$\begin{aligned} &D_{11}\frac{\partial^4 w_{12}^{(2)}}{\partial x^4} + 2(D_{12}+2D_{66})\frac{\partial^4 w_{12}^{(2)}}{r^2\,\partial\theta^2\,\partial x^2} + D_{22}\frac{\partial^4 w_{12}^{(2)}}{r^4\,\partial\theta^4} + \frac{1}{r}N_{\theta_{12}} + \lambda\left(\bar{N}_{x0}\frac{\partial^2 w_{12}^{(2)}}{\partial x^2} + \bar{N}_{\theta 0}\frac{\partial^2 w_{12}^{(2)}}{r^2\,\partial\theta^2}\right) \\ &\quad = -A_{22}\frac{w_1^{(1)}}{r}\frac{\partial^2 w_2^{(1)}}{r^2\,\partial\theta^2} = C\,w_m(x)w_n(x)\cos(m\theta)\cos(n\theta) \\ &\quad = \tfrac{1}{2}C\,w_m(x)[w_n(x)\cos(m+n)\theta + w_n(x)\cos(m-n)\theta]. \end{aligned} \tag{18}$$

D_{11}, D_{12} etc. are appropriate flexural stiffnesses (Jones, 1975). The left hand side of eqn (18) is of the same form as that of the eigenvalue problem, while the right side of it may be viewed as a loading term. In so far as $n \gg m$, the longitudinal description of $w_n(x)$ for the neighboring local modes associated with mode number $n-m$ and $n+m$ would be substantially the same, i.e. $w_{n-m}(x) \simeq w_n(x)$, $w_{n+m}(x) \simeq w_n(x)$. Thus the right hand side describes a loading system which is proportional to the normal deflections of two neighboring local modes and modulated by the function $w_m(x)$ in the longitudinal direction. The system of equations gives a response which is controlled by the magnitude of the loading parameter λ on the left hand side and belongs to the family of linear instability problems, where instability is triggered by some loading or imperfections. In the absence of odd derivatives on the left hand side the response would be in phase with the loading and would primarily contain the buckling modes corresponding to wave number $n-m$ and $n+m$ whose amplitudes would be modulated by $w_m(x)$. The solution would automatically satisfy the required orthogonality condition with respect to both the primary buckling modes by virtue of the trigonometric variations associated with it.

Now consider the solution as λ approaches the critical load corresponding to the local mode. Since for large n, the critical loads corresponding to wave numbers $n-m$ and $n+m$ are not likely to differ significantly from that of n, the participation of these modes is exaggerated because of the singularities associated with the neighboring modes of buckling. This will render the solution invalid and is a consequence of the way in which the problem is posed and solved, rather than the intrinsic nature of the problem.

In order to avoid this pitfall, one might recognize the neighboring modes associated with the wave numbers $n-m$ and $n+m$ as additional fundamental modes participating in the interaction. [Byskov (1983), (1988) discusses the effect of omitting the neighboring local modes in the analysis]. Thus we would have a problem of the interaction of one overall mode with three close local modes. However, the problem of singularities in the determination of the mixed second order field still exists because of the triggering row of the modes associated with wave numbers $n-2m$ and $n+2m$. Thus once again these modes would have to be treated as fundamental modes. The process must be continued till a cluster of local modes are accounted for as primary participating modes, i.e. those with wave numbers:

$$\cdots n-3m, \quad n-2m, \quad n-m, \quad n, \quad n+m, \quad n+2m, \quad n+3m \cdots .$$

Each of the mixed second order fields that arises by the interaction of the overall mode with a local mode can be evaluated taking into account the orthogonality condition between this field and all the local modes as well as the overall mode. Likewise, the mixed second order field that arises by the interaction of any two local modes must be rendered orthogonal to every local mode. Such a multi-modal interaction analysis does not seem to be attractive from the point of view of computational simplicity.

Now, a linear combination of several neighboring modes taken in the form:

$$\begin{Bmatrix} u_2^{(1)} \\ v_2^{(1)} \\ w_2^{(1)} \end{Bmatrix} = \cdots + a_{n-3m} \begin{Bmatrix} u_{n-3m}(x)\cos(n-3m)\theta \\ v_{n-3m}(x)\sin(n-3m)\theta \\ w_{n-3m}(x)\cos(n-3m)\theta \end{Bmatrix} + a_{n-2m} \begin{Bmatrix} u_{n-2m}(x)\cos(n-2m)\theta \\ v_{n-2m}(x)\sin(n-2m)\theta \\ w_{n-2m}(x)\cos(n-2m)\theta \end{Bmatrix} + \cdots \tag{19}$$

may be viewed as simply the local mode corresponding to wave number n modulated with respect to both the amplitude and phase. Thus the expression in eqn (19) may be written as:

$$\begin{Bmatrix} u_2^{(1)} \\ v_2^{(1)} \\ w_2^{(1)} \end{Bmatrix} = F(\theta) \begin{Bmatrix} u_n(x)\cos(n\theta+\psi(\theta)) \\ v_n(x)\sin(n\theta+\psi(\theta)) \\ w_n(x)\cos(n\theta+\psi(\theta)) \end{Bmatrix} \tag{20}$$

where $F(\theta)$ and $\psi(\theta)$ may be viewed as slowly varying functions providing for slowly varying amplitude and phase. Here we assume that $u_{n-m}(x) \simeq u_n(x)$, $u_{n+m}(x) \simeq u_n(x)$, etc. If in addition the contributions of a pair of local modes located symmetrically with respect to the primary local mode i.e. those having the wave number $n-m$, $n+m$ and $n-2m$, $n+2m, \ldots$ etc. can be assumed to be substantially the same, the function $\psi(\theta)$ may be neglected in eqn (20).

Now consider eqn (18) once again. The right hand side is seen to be proportional to the normal deflections of the local modes with wave numbers $n-m$ and $n+m$, modulated by a slowly varying function, *viz.*, $w_m(x)$. Thus the response must be in terms of the said local modes modulated by a slowly varying function in the x-direction. In view of this, the local mode is taken in a form whose amplitude varies slowly both in the circumferential and longitudinal directions. Thus the local buckling is represented in the form:

$$\begin{Bmatrix} u_2^{(1)} \\ v_2^{(1)} \\ w_2^{(1)} \end{Bmatrix} = G(x,\theta) \begin{Bmatrix} u_n(x)\cos(n\theta) \\ v_n(x)\sin(n\theta) \\ w_n(x)\cos(n\theta) \end{Bmatrix} \tag{21}$$

where $G(x,\theta)$ is as yet an unknown amplitude modulating function associated with the local mode and will be determined by a nonlinear analysis. It may be taken in the form:

$$G(x,\theta) = \sum_{i=0}^{N} \sum_{j=0}^{2} [a_{ij}^S \sin(im\theta) + a_{ij}^c \cos(im\theta)] g_j(x) \overset{def}{=} a_{ij} f_i(\theta) \phi_j(x) \tag{22}$$

where m is the number of waves of overall buckling, and $\phi_j(x)$ has been chosen as a linear function over each bay. N will be determined based on numerical convergence and is often a small number, 1 or 2. a_{ij} are the degrees-of-freedom depicting the amplitude modulation.

Such a representation not only simplifies the formulation of the problem but also eliminates the potential danger of singularities associated with the higher buckling modes in the immediate vicinity of the primary local mode. For now, the mixed second order field must be so determined as to be orthogonal to all the local modes comprehended in the right

hand side of eqn (21). (The latter are a set of local modes of variable wave numbers which include $n-m$ and $n+m$ but of the same x-variation as the primary local mode.) This orthogonality condition is discussed in the next section. The solution of the mixed second order field is no longer plagued by singularities, for it contains contributions in the form of neither the primary nor the neighboring local modes.

The mixed second order field. In this section, the evaluation of the mixed second order field is discussed. Even though the local mode is now amplitude-modulated and consists therefore of a number of neighboring local modes, we compute only that part of the mixed second order field which arises by the interaction of the overall mode (wave number m) with the primary local mode (wave number n). By invoking the full set of exact equilibrium equations, it is readily shown that the mixed second order displacement field for the general case of anisotropy may be represented in the form:

$$\begin{aligned} u_{12_k}^{(2)} &= u_{kij}^{2S*}\Phi_i(\zeta)\Phi_j(\eta)\sin(n-m)\theta + u_{kij}^{2C*}\Phi_i(\zeta)\Phi_j(\eta)\cos(n-m)\theta \\ &+ u_{kij}^{2S**}\Phi_i(\zeta)\Phi_j(\eta)\sin(n+m)\theta + u_{kij}^{2C**}\Phi_i(\zeta)\Phi_j(\eta)\cos(n+m)\theta \\ &(i=1,2,\cdots,p_r+1;\quad j=1,2,\cdots,p_x+1;\quad k=1,2,3). \end{aligned} \tag{23}$$

The orthogonality condition is therefore so set up as to preclude the appearance of the modes corresponding to wave numbers, $n-m$ and $n+m$ as part of the mixed second order field. The orthogonality condition is taken in the same form as for two buckling modes of the structure, i.e. in the form:

$$\sigma_i^{(0)} \cdot \mathrm{L}_{11_j}(u_{2_j}^{(1)}, u_{12_j}^{(2)}) = 0 \quad (i=1,2,\cdots,6;\quad j=1,2,3). \tag{24}$$

It is now possible to set up the potential energy functional governing the mixed second order field (Benito and Sridharan, 1985) which is rendered stationary under the constraint of the orthogonality condition; the Lagrange multiplier technique will be used to achieve this. The functional may be written in the form:

$$\begin{aligned} \Pi_{12}^{(2)} &= \tfrac{1}{2}C_{ij}\{\mathrm{L}_{1_{ik}}(u_{12_k}^{(2)})\cdot\mathrm{L}_{1_{jl}}(u_{12_l}^{(2)}) + 2[\mathrm{L}_{1_{ik}}(u_{12_k}^{(2)})\cdot\mathrm{L}_{11_j}(u_{1_l}^{(1)}, u_{2_l}^{(1)}) \\ &+ \mathrm{L}_{1_{jk}}(u_{1_k}^{(1)})\cdot\mathrm{L}_{11_j}(u_{2_l}^{(1)}, u_{12_l}^{(2)}) + \mathrm{L}_{1_{ik}}(u_{2_k}^{(1)})\cdot\mathrm{L}_{11_j}(u_{1_l}^{(1)}, u_{12_l}^{(2)})]\} \\ &+ \tfrac{1}{2}\lambda\sigma_i^{(0)}\cdot\mathrm{L}_{2_{ik}}(u_{12_k}^{(2)}) + \Lambda\sigma_i^{(0)}\cdot\mathrm{L}_{11_1}(u_{2_k}^{(1)}, u_{12_k}^{(2)})(i,j=1,2,\cdots,6;\quad k,l=1,2,3) \end{aligned} \tag{25}$$

where a Λ is the unknown Lagrangian multiplier. Substituting eqn (23) into eqn (25), the mixed second order displacement fields are generated by rendering the potential energy function stationary, λ being set equal to a smaller critical load such that $\lambda = \min(\lambda_1, \lambda_2)$ which respectively represent overall and local critical load. Because of orthogonality condition with respect to the trigonometric terms, there exists no coupling between single and double asterisk quantities in eqn (23). Thus these two displacement fields can be obtained by the respective uncoupled analysis.

Potential energy function. All the displacement fields required to deal with the interaction problem are now obtainable so that one could formulate the potential energy function in terms of scalar parameters ξ_1 and ξ_2. A scalar parameter ξ_2 is now replaced by a slowly varying function defined by eqn (22) as to account for amplitude modulation of the local mode. With an understanding of neglect of the prebuckling deformation, eqn (16) will be expressed as:

$$\begin{aligned} \{u\} &= \{u_1^{(1)}\}\xi_1 + \{u_2^{(1)}\}f_i(\theta)\phi_j(x)\xi_{ij} + \{u_{11}^{(2)}\}\xi_1^2 \\ &+ \{u_{12}^{(2)}\}f_i(\theta)\phi_j(x)\xi_{ij}\xi_1 + \{u_{22}^{(2)}\}f_i(\theta)\phi_j(x)f_k(\theta)\phi_l(x)\xi_{ij}\xi_{kl} + \cdots. \end{aligned} \tag{26}$$

The effects of initial imperfections u which may be taken as a linear combination of the modes of buckling may be represented as:

$$\{\tilde{u}\} = \{u_1^{(1)}\}\tilde{\xi}_1 + \{u_2^{(1)}\}f_i(\theta)\phi_j(x)\tilde{\xi}_{ij} \tag{27}$$

in which ξ_1 and ξ_{ij} are imperfection parameters. By using the relevant nonlinear strain–displacement relations and the constitutive matrix, the potential energy function of the imperfect structure is expressed in terms of ξ_1 and ξ_{ij}, but truncated at quartic terms in ξ_1 and ξ_{ij}. Simplification in setting up the potential energy function is achieved by the use of (i) the orthogonality of the trigonometric functions associated with matrices relating strains and the degrees-of-freedom and (ii) the fact that the wave length of the local mode is considerably smaller than that of the overall mode; this permits the integrations for the local and overall quantities to be performed independently.

Referring to eqn (26), strain components including the nonlinear part may be decomposed in the form of trigonometric series in the following manner, taking for example $N = 1$ in Eqn (22):

$$\begin{aligned}\{\varepsilon\} = \{\varepsilon_0\} &+ \sum_{i=1}^{2} [\{\varepsilon_i^{Sm}\} \sin im\theta + \{\varepsilon_i^{Cm}\} \cos im\theta + \{\varepsilon_i^{Sn}\} \sin in\theta + \{\varepsilon_i^{Cn}\} \cos in\theta] \\ &+ \sum_{i=1}^{2}\sum_{j=1}^{2} [\{\varepsilon_{ij}^{SSmn}\} \sin im\theta \sin jn\theta + \{\varepsilon_{ij}^{SCmn}\} \sin im\theta \cos jn\theta \\ &+ \{\varepsilon_{ij}^{CSmn}\} \cos im\theta \sin jn\theta + \{\varepsilon_{ij}^{CCmn}\} \cos im\theta \cos jn\theta] \quad (m \neq n).\end{aligned} \tag{28}$$

By inspection each component is orthogonal to the others. The total potential energy function governing interactive buckling is then obtained by summing up all contributions to eqn (28) (see Kasagi, 1994 for details). This may be symbolically expressed as follows:

$$\begin{aligned}\Pi = \frac{1}{2}\sum_i \int_v \{\varepsilon\}_i^T [C]\{\varepsilon\}_i \, dv = &-\lambda b_1 \xi_1 \tilde{\xi}_1 - \lambda b_{ijkl}\xi_{ij}\tilde{\xi}_{kl} + \tfrac{1}{2}(a_1 - \lambda b_1)\xi_1^2 + d_1\xi_1^4 \\ &+ \tfrac{1}{2}(a_{ijkl} - \lambda b_{ijkl})\xi_{ij}\xi_{kl} + d_{ijklpqrs}\xi_{ij}\xi_{kl}\xi_{pq}\xi_{rs} + e_{ijkl}\xi_{ij}\xi_{kl}\xi_1 + g_{ijkl}\xi_{ij}\xi_{kl}\xi_1^2\end{aligned} \tag{29}$$

where $a_1, b_1, \cdots g_{ijkl}$ are constants.

Classification of nonlinear interaction terms. In eqn (29) the terms which involve e_{ijkl} and g_{ijkl} are the nonlinear interaction terms. The former is a family of cubic terms and in the presence of small imperfections would be of far greater significance than the latter which is a family of quartic terms. The former has a destabilizing influence whereas the latter turns out to be mildly stabilizing in character. It is also important to note that the cubic terms which play such a pivotal role in the interaction would have vanished but for the amplitude modulation—as has been observed by Koiter (1976b) in a general context. For the purpose of discussion of the relative significance of the various interaction terms, it is expedient to classify them in the following manner:

(i) Cubic terms (Q_3):

The non-vanishing terms in this group arise from the first order overall strains (stresses) working over quadratic contributions of the first order local stresses (strains).

(ii) Quartic terms (Q_4):

These consist of the interactions of the first and second order strains (stresses) of individual mode with those of the other. No mixed second order strains such as $L_{11}(u_1^{(1)}, u_2^{(1)})$ are included here.

(iii) Mixed second order terms (Q_{mix}):

These consist of all terms that would arise by the interaction of the mixed second strains and stresses with each other. The mixed second order strain can be expressed in the form:

$$\varepsilon_{12}^{(2)} = \mathrm{L}_1(u_{12}^{(2)}) + \mathrm{L}_{11}(u_1^{(1)}, u_2^{(1)}).$$

It must be emphasized that in developing the potential energy function the two terms in the foregoing should be taken together or neglected together in a consistent formulation.

Further description of each of the three terms is given in Appendix C.

3. NUMERICAL EXAMPLES AND DISCUSSION

Before proceeding to the analysis of modal interaction, buckling and postbuckling analysis of both local and overall modes must be done individually in order to determine the respective buckling modes and associated second order fields. Nonlinear equations of equilibrium derived from the functional given by eqn (29) are expressed in terms of the current value of the load parameter and the degrees-of-freedom depicting the amplitude modulating function as well as the amplitude of the overall mode. The structural response is traced by the constant arc length scheme (Crisfield, 1981) coupled with equilibrium iteration.

Two types of cylinders having stacking sequences $[90/0]_S$ (Family #1) and $[45/-45]_{QS}$ (Family #2) for shell skins are considered. In both cases the stiffeners are assumed to be made up of $[90/0]_S$ laminates. The end boundary conditions are assumed to be simply supported. The material properties are given as follows (in psi if applicable):

$$E_{11} = 16\times10^6 E_{22} = E_{33} = 1.48\times10^6 \quad G_{12} = G_{13} = 0.76\times10^6$$

$$G_{23} = 0.51\times10^6 \quad \nu_{12} = \nu_{13} = 0.33 \quad \nu_{23} = 0.45.$$

We define the volume ratio ρ such as:

$$\rho = V_{\text{stiff}}/V_{\text{total}}$$

in which V_{total} is the total volume of material used for the shell including stiffeners whereas V_{stiff} is that of stiffeners alone. In the present study, V_{total} and ρ are kept constant as the number of stiffeners N_S and the depth of the stiffeners d are varied. Table 1 presents the

Table 1. Buckling pressure and postbuckling response of the stiffened shells, $R = 50$ in. (Dominant mode of buckling underlined)

(a) $[90/0]_S$ shells, $L/R = 2.62$, $R/h = 100$, $t_S/h = 2.0$, $\rho = 28\%$

			Overall mode			Local mode			
N_S	d/t_S	S_p/R	$\lambda_1\times10^5$	(m)	$\lambda^{(2)}$	$\lambda_2\times10^5$	(n)	$\lambda^{(2)}$	λ_2/λ_1
8	3.414	0.274	2.49	3	+0.010	<u>1.48</u>	10	−0.106	0.59
9	3.022	0.244	2.15	3		<u>1.69</u>	10		0.79
10	2.711	0.220	1.90	3	−0.007	<u>1.89</u>	10	−0.047	0.99
11	2.458	0.200	<u>1.71</u>	3		2.10	10		1.23
12	2.248	0.183	<u>1.57</u>	3	−0.002	2.30	10	+0.005	1.46

(b) $[45/-45]_{QS}$ shells, $L/R = 4.64$, $R/h = 62.5$, $t_S/h = 1.5$, $\rho = 27\%$

			Overall mode			Local mode			
N_S	d/t_S	S_p/R	$\lambda_1\times10^5$	(m)	$\lambda^{(2)}$	$\lambda_2\times10^5$	(n)	$\lambda^{(2)}$	λ_2/λ_1
8	6.708	0.494	5.77	2	−0.106	<u>3.22</u>	10	−0.353	0.56
9	5.900	0.442	5.04	2		<u>3.88</u>	11		0.77
10	5.267	0.400	<u>4.58</u>	2	−0.054	4.59	11	−0.518	1.00
11	4.756	0.365	<u>4.27</u>	2		5.39	11		1.26
12	4.337	0.335	<u>4.03</u>	2	−0.023	6.23	12	−0.708	1.55

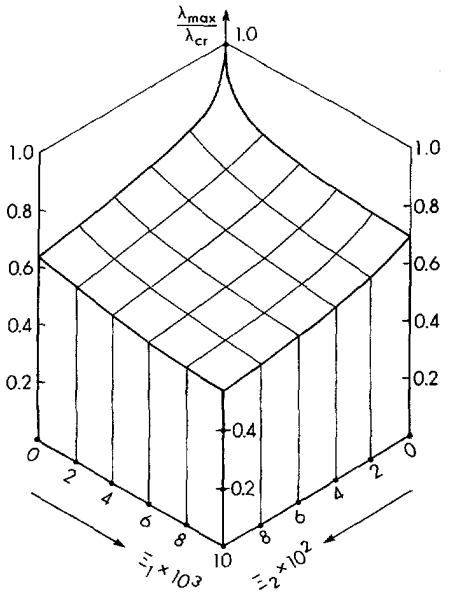

Fig. 3(a). Imperfection-sensitivity surface of the $[90/0]_S$ composite shell (Family #1, $N_S = 10$).

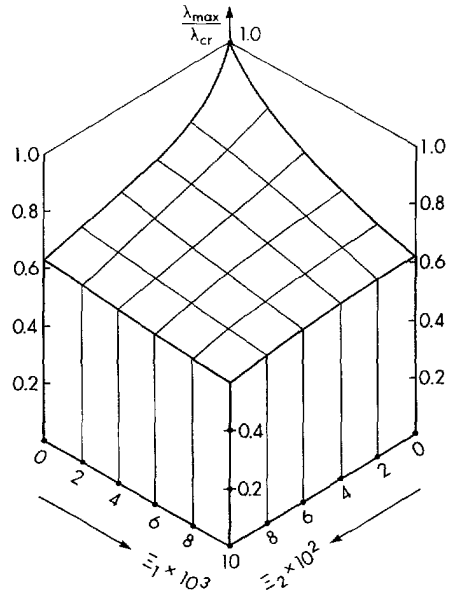

Fig. 3(b). Imperfection-sensitivity surface of the $[45/-45]_{QS}$ composite shell (Family #2, $N_S = 10$).

geometric parameters (Fig. 2(a–b) as key). All the computations are performed with p-levels, $p_r = 2$ and $p_x = 5$ for both local and overall buckling analysis. Table 1 gives the buckling pressures associated with local and overall buckling as well as the imperfection-sensitivity in the respective mode of buckling. It is seen that the shell having ten stiffeners ($N_S = 10$) is the case where two critical pressures are coincident, triggering both the local and the overall modes simultaneously.

The amplitude modulating function $[G(x, \theta)]$ is considered to vary linearly over each day for the longitudinal description, but assumed to be constant over the junction element connecting the shell with stiffeners. It was found sufficient to consider terms up to $N = 1$ of the trigonometric series characterizing the amplitude modulation function around the circumference in eqn (22). The amplitude of initial imperfections are expressed in dimensionless forms by division by the radius and the thickness of the shell for overall and local

imperfections respectively. A dimensionless load parameter λ is obtained by dividing the pressure by E_{11}. Then λ_1 and λ_2 are the critical values of λ for overall and local buckling respectively.

Imperfection-sensitivity surface. This section deals with the case of simultaneous buckling which highlights the main features of interactive buckling. Figure 3(a–b) gives the imperfection-sensitivity surface for coincident buckling ($N_S = 10$), showing the maximum load carrying capacity, λ_{max}, for a given combination of imperfection parameters. If any one of the two imperfection parameters is set to zero, i.e. along the paths $\Xi_1 = 0$ or $\Xi_2 = 0$, the primary solution path loses the stability by bifurcation at a point where a secondary coupled equilibrium path (exhibiting deformation in both the modes) intersects it. These figures indicate severe load reduction of load carrying capacity λ_{max} in the range of small imperfections. In contrast, the rate of load reduction becomes smaller as imperfection magnitudes are increased.

The stiffened shells undergoing primarily local buckling exhibit a rather interesting phenomenon as revealed by the present nonlinear analysis. It is not surprising that amplitude modulation of the local buckling mode does occur in a significant way because of the interaction with the overall mode. But it is found that even with the action of overall buckling completely suppressed ($\xi_1 = 0$), there occurs some noticeable variation of the amplitude along the length of the shell. This is due to the variation of the axisymmetric deformation (second order field) along the length of the shell, which causes the shell near the supports to buckle inward. This amplitude modulation by itself can account for a certain reduction in the load carrying capacity in comparison to that predicted by the asymptotic local buckling analysis.

Influence of the various coupled terms. A relatively simple interaction analysis is possible considering (Q_3) terms alone in the potential energy function. If one seeks a more accurate prediction of the structural response, it is necessary to take quartic interaction terms (Q_4) into account in the potential energy function; further refinement is possible considering the terms associated with the mixed second order field (Q_{mix}). Figure 4 presents the effects of quartic terms and the mixed second order field for the same shell as in Fig. 3(a), evaluated along a coupled path $\Xi_1 \times 10 = \Xi_2$. It is seen that the contribution of the quartic terms (Q_4) makes a difference in the range of large imperfections and has a tendency to stabilize the structure; however, this effect is quite minor. The terms associated with the mixed second order field (Q_{mix}) give negligibly small contributions to the structural response in comparison to the cubic (Q_3) and quartic (Q_4) terms. It appears that the amplitude modulation function is capable of describing the major effects of the changes of deformation arising out of interaction. It follows that the incorporation of this field into the analysis may no longer be necessary from a practical standpoint.

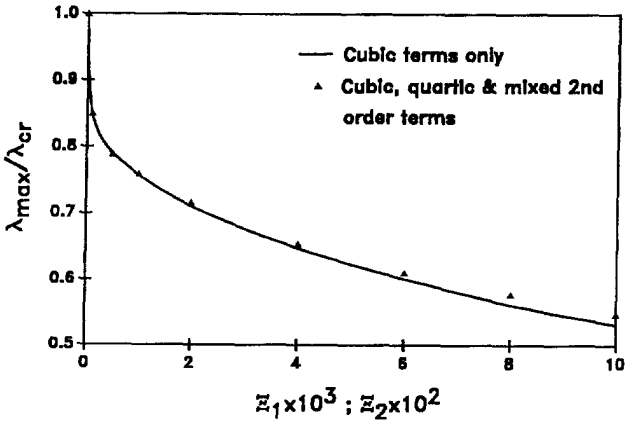

Fig. 4. Effects of the quartic and the mixed second order field for the $[90/0]_S$ composite shell (Family #1, $N_S = 10$) along the path $\zeta_1 \times 10 = \zeta_2$.

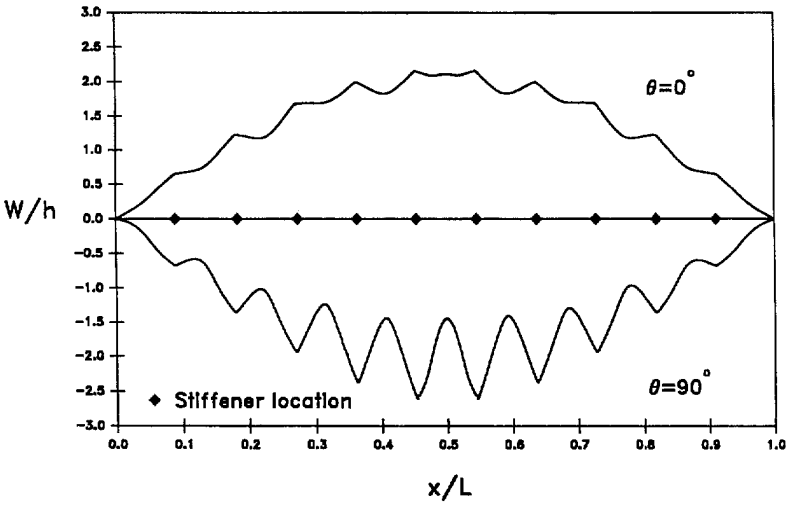

Fig. 5(a). Longitudinal description of deformation patterns of the $[45/-45]_{QS}$ composite shell (Family #2, $N_S = 10$), $\zeta_1 = 0.01$, $\zeta_2 = 0.1$.

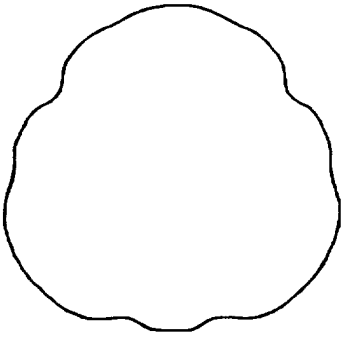

Fig. 5(b). Cross-sectional deformation pattern of the $[90/0]_S$ composite shell (Family #1, $N_S = 10$) $\zeta_1 = 0.01$ and $\zeta_2 = 0.1$.

Deformation patterns. The longitudinal variation of radial displacement (Family #2, $N_S = 10$) is depicted in Fig. 5(a) taking imperfection parameters $\Xi_1 = 0.01$ and $\Xi_2 = 0.1$ at the limit point. The amplitude of local mode is modulated so that the waves almost vanish in the tensile portions of overall mode at the center, at $\theta = 0°$ or 180°. Nevertheless the shell has a strong tendency to buckle inward between stiffeners. Turning our attention to the compressive part of the overall mode at $\theta = 90°$ or 270°, stiffeners carry much of the compression and buckle inward even more severely than the shell portions between them. Deformation shapes of cross section (Family #1, $m = 3$, $N_S = 10$) are shown in Fig. 5(b) which is obtained at the limit point. Note that the local buckles on the tension side of overall buckling are mitigated and those on the compression side are accentuated. A similar effect is seen in the longitudinal profile of the deformed shell.

Interlaminar stresses. The interlaminar stresses play a key role in precipitating a delamination type of failure in composite shells. It is found that the magnitude of transverse shearing stresses is far higher than the normal stress σ_{rr}, because of the slow variation of the displacement gradient in the radial direction; attention is therefore focused on the former in the sequel. Figure 6(a–b) plots the stresses $\tau_{r\theta}$ and τ_{rx} versus a load parameter λ. The interlaminar stresses are evaluated at a location where the respective components take the maximum values: $\tau_{r\theta}$ is at the center of the shell while τ_{rx} is at the junction to a stiffener nearest from the center. The two figures show similar characteristics; the rate of growth of the stress increases drastically in the vicinity of the load limit point. Because Family #2

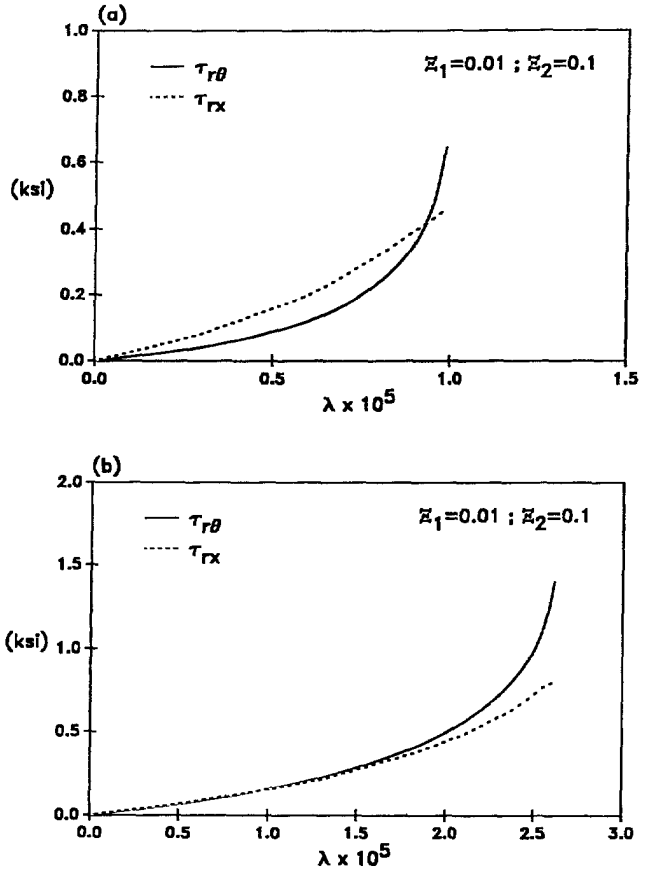

Fig. 6. Maximum interlaminar stresses. (a) The $[90/0]_S$ composite shell (Family #1, $N_S = 10$); (b) the $[45/-45]_{QS}$ composite shell (Family #2, $N_S = 10$).

are thicker shells than Family #1, the interlaminar stresses play a more significant role in the former.

Prediction of delamination and material failure are beyond the scope of the present paper. If delamination does occur, the material failure would be expected to initiate in the central region, in particular at the shell–stiffener junction.

Volume change of shell. Another important aspect of shell response is the relation between the volumetric strain $\Delta V/V_0$ and a load parameter λ. V_0 is the shell volume at the undeformed state, and ΔV represents a change in volume. In tests on shells subject to hydrostatic pressure, volume control is often the mode of load application. As soon as the maximum pressure is reached, the shell undergoes a dynamic snap-through buckling to a remote equilibrium state (see for example, Thompson and Hunt, 1984). Figure 7 gives pressure–volume change characteristics of a shell of Family #1 under interactive buckling. It is found that the response becomes sharply re-entrant at the maximum load and thus the snap-through buckling is inevitable. The present formulation, because of its asymptotic character, is not satisfactory in the advanced post buckling ranges and, therefore, the characteristics are not traced well into the unloading regime; the analysis just predicts the direction of the equilibrium path in the initial post-collapse range. In any case, in either mode of loading—pressure control or volume control—the analysis strongly indicates a catastrophic collapse.

Spectra of imperfection-sensitivity. In this section the imperfection-sensitivity of shells is discussed with the ratio of the critical pressures λ_2/λ_1 varied over a rather wide range. For a given total volume of the shell and geometric proportions of the stiffeners, the number of stiffeners N_S controls the ratio of critical pressures. Figure 8(a–b) presents curves of

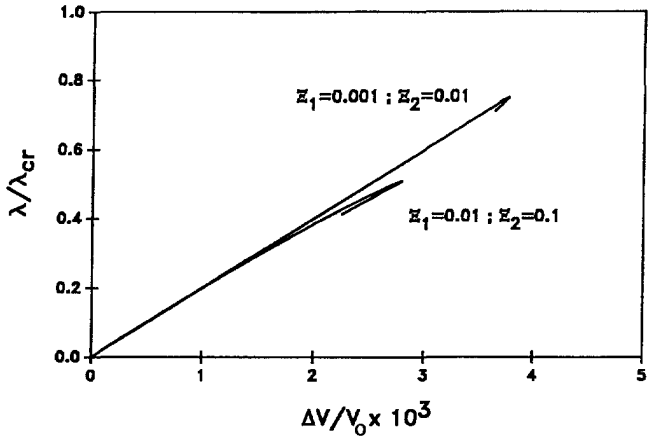

Fig. 7. Pressure–volumetric strain characteristics of the $[90/0]_S$ composite shell (Family #1, $N_S = 10$).

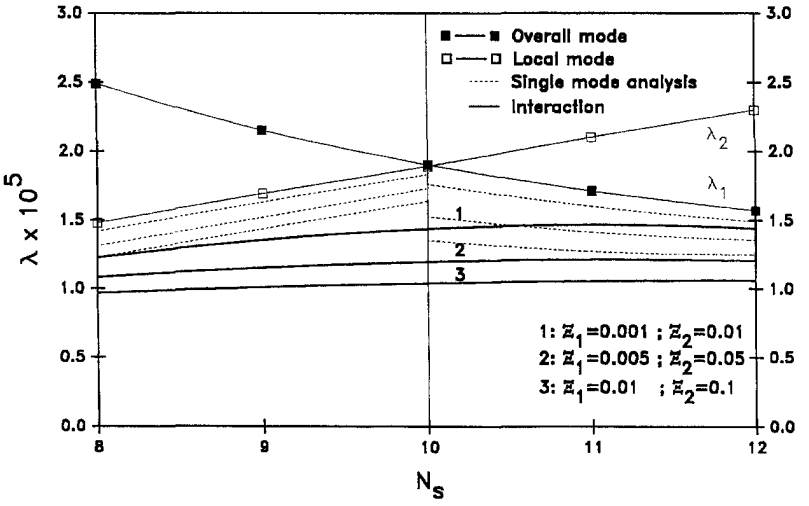

Fig. 8(a). Imperfection-sensitivity spectra of the $[90/0]_S$ composite shells (Family #1).

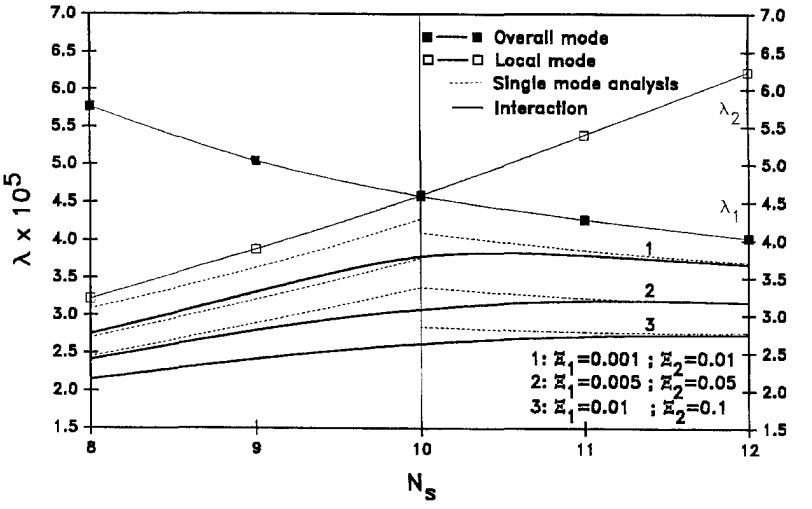

Fig. 8(b). Imperfection-sensitivity spectra of the $[45/-45]_{QS}$ composite shells (Family #2).

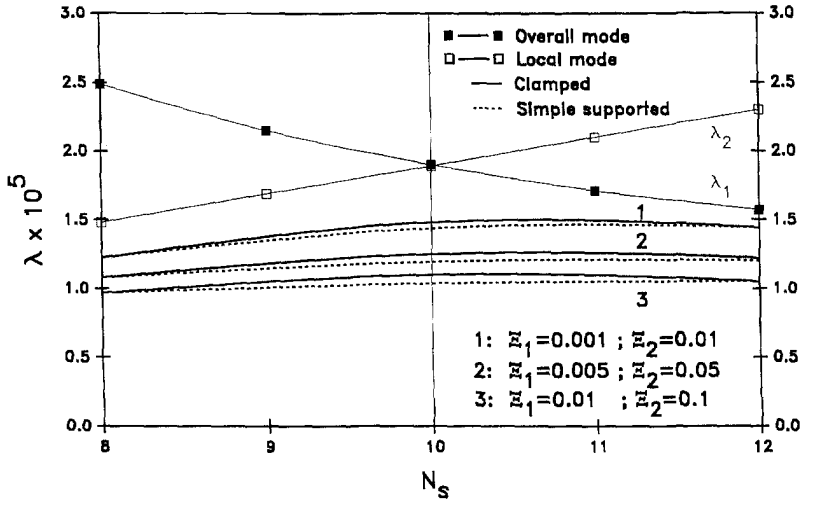

Fig. 8(c). Comparison of imperfection-sensitivity spectra of the $[90/0]_S$ composite shells (Family #1).

imperfection spectra where the curves marked by λ_1 and λ_2 indicate the critical loads of respective buckling modes, see Table 1. As indicated, three levels of combinations of imperfection parameters are considered in the illustration. The dashed lines give the maximum loads attainable without the interaction as given by the asymptotic analysis [eqn (15)].

The figures confirm the essential feature of stiffened shell behavior—they are very imperfection-sensitive in the range where λ_1 and λ_2 are close to each other. In this region the interaction curves lie much below the dashed lines. Imperfection-sensitivity is rather more severe in the region in which the local buckling load is smaller than the overall one. Such an observation is consistent with the fact that the type of the shells considered here possesses a much higher negative postbuckling coefficient $\lambda^{(2)}$ with respect to local buckling than the one corresponding to overall buckling. Note further that the dashed lines plot only the results based on the asymptotic procedure that does not account for amplitude modulation—something which occurs for the case of local buckling even in the absence of the interaction. The interaction curves reveal that as the imperfections increase, the maximum load attainable shifts toward the region where $\lambda_1 < \lambda_2$. Thus an optimum point exists on the side in which $N_S > 10$, thus moving away from the simultaneity point. Imperfection-sensitivity under overall mode buckling is much smaller than that in local buckling. The optimal value of N_S is located in the region where the overall mode is the governing mode.

Figure 8(c) shows a comparison of the imperfection-sensitivity spectra for two types of end conditions, *viz.* simply supported and clamped. Family #1 is studied here. All the parameters are the same for the two types of shell except for the change of end conditions. In general, a clamped shell has a higher buckling load against overall mode [not shown in Fig. 8(c)], but the support condition is immaterial for the local mode. It is seen that the clamped shells are less imperfection-sensitive than simply supported shells.

The effects of interaction are most significant in the range of critical stress ratios (λ_2/λ_1) of $\frac{1}{2}$ to 2. In this range the reduction of the load carrying capacity can be as high as 50% for imperfections of such magnitude as may be unavoidable in practice. Imperfection spectra reveal that a design based on classical "naive" criteria is not necessarily optimal. There are clear advantages in making the local critical pressure higher than the overall critical pressure by 50% $(\lambda_2/\lambda_1 \simeq 1.5)$. Such shells are clearly less imperfection-sensitive than those with coincident critical values and thus retain much of their capacities in the presence of imperfections. Furthermore, the severe interlaminar stresses accompanied with local buckling are absent.

Acknowledgement—The present work has been supported by the Office of Naval Research Grant No. N00014-91-J1637. The authors are grateful to Dr Yapa D. S. Rajapakse, the director of the Solid Mechanics program for his keen interest in the work and constant encouragement to the authors.

REFERENCES

Ambartsumyan, S. A. (1970). *Theory of Anisotropic Plates*. Technomic Publishing, Westport, CO.
Bathe, K.-J. (1982). *Finite Element Procedures in Engineering Analysis*. Prentice–Hall, Englewood Cliffs.
Benito, R. and Sridharan, S. (1985). Interactive buckling analysis with finite strips. *Int. J. Num. Meth. Eng* **21**, 145–161.
Brush, D. O. and Almroth, B. O. (1975). *Buckling of Bars, Plates, and Shells*. McGraw–Hill, New York.
Byskov, E. (1983). An asymptotic expansion applied to van der Neut's column. In *Collapse* (Edited by J. M. T. Thompson and G. W. Hunt), pp. 269–281. Cambridge University Press, Cambridge, England.
Byskov, E. (1988). Elastic buckling with infinitely many local modes. *Mech. Struct. Mach.* **15**(4), 413–435.
Byskov, E., Damkilde, L. and Jensen, K. J. (1988). Multimode interaction in axially stiffened cylindrical shells. *Mech. Struct. Mach.* **16**(3), 387–405.
Byskov, E. and Hanson, J. C. (1980). Postbuckling and imperfection-sensitivity analysis of axially stiffened cylindrical shells with mode interaction. *J. Struct. Mech.* **8**(2), 205–224.
Byskov, E. and Hutchinson, J. W. (1977). Mode interaction in axially stiffened cylindrical shells. *AIAA J.* **15**(7), 941–948.
Crisfield, M. A. (1981). A fast incremental/iterative solution procedure that handles "snap-through". *Comput. Struct.* **13**, 55–62.
Hui, D. (1985). Amplitude modulation theory and its applications to two-mode buckling problems. *J. Appl. Math. Phys. (ZAMP)* **35**, 789–802.
Jones, R. M. (1975). *Mechanics of Composite Materials*. Hemisphere Publishing, New York.
Kardomateas, G. A. (1993). Buckling of orthotropic cylindrical shells under external pressure. *J. Appl. Mech. ASME* 195–202.
Kasagi, A. (1994). Interactive buckling of ring stiffened composite cylindrical shells. D. Sc. Thesis, Department of Civil Engineering, Washington University, St Louis, MO.
Kasagi, A. and Sridharan, S. (1993). Buckling and postbuckling analyses of thick composite cylindrical shells under hydrostatic pressure using axisymmetric solid elements. *Comp. Engng* **3** (5), 467–487.
Kasagi, A. and Sridharan, S. (1994). Imperfection-sensitivity of layered composite cylindrical shells. Submitted to *J. Engng Mech. ASCE*.
Koiter, W. T. (1945). *On the Stability of Equilibrium*. Delft, Holland. (English Translation: NASA, Tech. Trans., 1967, F-10, 833).
Koiter, W. T. (1967). General equations of elastic stability for thin shells. In Proceedings of the Symposium on the Theory of Shells to Honor Lloyd Hamilton Donnell. University of Houston, TX, 187–228.
Koiter, W. T. and Pignataro, M. (1976a). A general theory of the interaction between local and overall buckling in stiffened panels. Delft University of Technology, Report WTHD-83, Delft, The Netherlands.
Koiter, W. T. and Pignataro, M. (1976b). General theory of mode interaction in stiffened plate and shell structures. Delft University of Technology, Report WTHD-91, Delft, The Netherlands.
Koiter, W. T. and Skaloud, M. (1963). Interventions, comportment postcritique des plaques utilisées en construction métallique. In *Mémoires de la Société Royale des Sciences de Liège*, 5^{me} Série (tome VIII, fasc. 5), 64–68, 103, 104.
van der Neut, A. (1969). The interaction of local buckling and column failure of thin-walled compression members. In *Proceedings of the 12th International Congress on Applied Mechanics*, pp. 389–399 Springer–Verlag, Berlin.
Simitses, G. J. and Anastasiadis, J. S. (1992). Shear deformable theories for cylindrical laminates—equilibrium and buckling with applications. *AIAA J.* **30**(3), 826–834.
Simitses, G. J., Tabiei, A. and Anastasiadis, J. S. (1993). Buckling of moderately thick laminated cylindrical shells under lateral pressure. *Comp. Engng* **3**(5), 409–417.
Sridharan, S. and Peng, M.-H. (1989). Performance of axially compressed stiffened panels. *Int. J. Solids Structures.* **25**(8), 879–899.
Szabó, B. A. and Babuska, I. (1991). *Finite Element Analysis*. John Wiley & Sons, New York.
Thompson, J. M. T. and Hunt, G. W. (1984). *Elastic Instability Phenomena*. John Wiley & Sons, New York.
Tvergaard, V. (1973). Influence of post-buckling behavior on optimum design of stiffened panels. *Int. J. Solids Structures* **9**, 1519–1534.

APPENDIX A: FLUID PRESSURE LOADING

The fluid pressure loading condition is such that the pressure at every point on the shell surface remains normal to the deformed surface. The potential function is derived as the work done by the external pressure working through the change in volume of the cylinder. The change in volume ΔV is given by:

$$\Delta V = \int\int\left[w + \frac{1}{2}\left\{w\left(\frac{\partial u}{\partial x}\right) - \left(\frac{\partial w}{\partial x}\right)u\right\} + \frac{1}{2R_1}\left\{v^2 - v\left(\frac{\partial w}{\partial \theta}\right) + \left(\frac{\partial v}{\partial \theta}\right)w + w^2\right\}\right] R_1 \, dx \, d\theta. \tag{A1}$$

In setting up the potential energy function for the buckled state, the linear term in eqn (A1) vanishes and only quadratic terms remain. Consequently the potential energy due to the fluid pressure Ω is given by:

$$\Omega = \frac{1}{2} q_0 \int\int\left[w\left(\frac{\partial u}{\partial x}\right) - \left(\frac{\partial w}{\partial x}\right)u + \frac{1}{R_1}\left[v^2 - v\left(\frac{\partial w}{\partial \theta}\right) + \left(\frac{\partial v}{\partial \theta}\right)w + w^2\right]\right] R_1 \, dx \, d\theta. \tag{A2}$$

APPENDIX B: p-VERSION SHAPE FUNCTIONS

The displacement functions, ϕ_i are defined in terms of a dimensionless coordinate $\zeta(-1 \leqslant \zeta \leqslant 1)$ and are taken in the form:

$$\phi_1 = \tfrac{1}{2}(1-\zeta)$$

$$\phi_2 = \tfrac{1}{2}(1+\zeta)$$

$$\phi_i = \psi_{i-1} \quad (i = 3, 4, \ldots, p+1) \tag{B1–3}$$

where

$$\psi_i(\zeta) = \sqrt{\frac{2i-1}{2}} \int_{-1}^{x} \mathrm{P}_{i-1}(t)\,\mathrm{d}t. \tag{B4}$$

P_i are the Legendre polynomials given by:

$$P_n(x) = \frac{1}{2^n n!}\frac{d^n}{\mathrm{d}x^n}(x^2-1)^n \tag{B5}$$

which have orthogonality properties. The higher degree polynomials ϕ, up to the fifth degree are given explicitly as follows:

$$\phi_3(\zeta) = \frac{\sqrt{6}}{4}(\zeta^2-1)$$

$$\phi_4(\zeta) = \frac{\sqrt{10}}{4}(\zeta^3-\zeta)$$

$$\phi_5(\zeta) = \frac{\sqrt{14}}{8}(5\zeta^4-6\zeta^2+1)$$

$$\phi_6(\zeta) = \frac{\sqrt{18}}{16}(7\zeta^5-10\zeta^3+3\zeta). \tag{B6–9}$$

APPENDIX C: NONLINEAR COUPLED TERMS IN THE POTENTIAL ENERGY FUNCTION

Cubic and quartic interaction terms in the potential energy function in eqn (34) are expressed as follows:

(I) Cubic terms (Q_3):

$$Q_3 = \tfrac{1}{2}[C]\mathrm{L}_1(u_1^{(1)}) \cdot \mathrm{L}_2(u_2^{(1)}). \tag{C1}$$

(II) Quartic terms (Q_4):

$$Q_4 = \tfrac{1}{2}[C][\mathrm{L}_2(u_1^{(1)}) \cdot \{\mathrm{L}_1(u_2^{(2)}) + \tfrac{1}{4}\mathrm{L}_2(u_2^{(1)})\} + \mathrm{L}_2(u_2^{(1)}) \cdot \{\mathrm{L}_1(u_1^{(2)}) + \tfrac{1}{4}\mathrm{L}_2(u_1^{(1)})\} + \mathrm{L}_1(u_2^{(2)}) \cdot \mathrm{L}_1(u_1^{(2)})]. \tag{C2}$$

(III) Mixed second order terms (Q_{mix}):

$$Q_{\mathrm{mix}} = Q_3 + Q_4$$

in which

$$\bar{Q}_3 = [C]\mathrm{L}_1(u_2^{(1)}) \cdot \mathrm{L}_{11}(u_1^{(1)}, u_2^{(1)}) \tag{C3}$$

$$\begin{aligned}\bar{Q}_4 = {} & \tfrac{1}{2}[C][\mathrm{L}_1(u_{12}^{(2)}) \cdot \mathrm{L}_1(u_{12}^{(2)}) + 2\{\mathrm{L}_1(u_{12}^{(2)}) \cdot \mathrm{L}_{11}(u_1^{(1)}, u_2^{(1)}) + \mathrm{L}_1(u_1^{(1)}) \cdot \mathrm{L}_{11}(u_2^{(1)}, u_{12}^{(2)}) \\ & + \mathrm{L}_1(u_2^{(1)}) \cdot \mathrm{L}_{11}(u_1^{(1)}, u_{12}^{(2)}) + \mathrm{L}_1(u_1^{(1)}) \cdot \mathrm{L}_{11}(u_1^{(1)}, u_2^{(2)}) + \mathrm{L}_1(u_2^{(1)}) \cdot \mathrm{L}_{11}(u_2^{(1)}, u_1^{(2)})\} \\ & + \mathrm{L}_{11}(u_1^{(1)}, u_2^{(1)}) \cdot \mathrm{L}_{11}(u_1^{(1)}, u_2^{(1)})] + \min(\lambda_1, \lambda_2)\sigma^{(0)} \cdot [\mathrm{L}_2(u_{12}^{(2)}) + \mathrm{L}_{11}(u_1^{(2)}, u_2^{(2)})].\end{aligned}$$

In the above equations $[C]$ is the matrix of constitutive relations.